

Viscous dissipation pattern in incompressible Newtonian simple shear zones: an analytical model

Soumyajit Mukherjee · Kieran F. Mulchrone

Received: 11 October 2012 / Accepted: 23 February 2013 / Published online: 12 March 2013
© Springer-Verlag Berlin Heidelberg 2013

Abstract An analytical model of shear heating in an inclined simple shear zone with Newtonian rheology under a reverse shear sense and an upward resultant pressure gradient is presented. Neglecting a number of secondary factors, the shear heat is expressed as a function of the total slip rates at the boundaries, pressure gradient, dip and thickness of the shear zone, and density, viscosity, and thermal conductivity of the rock. A quartic temperature profile develops with a point of maximum temperature near the bottom part of the shear zone in general. The profile is parabolic if pressure gradient vanishes leading to a Couette flow. The profile attains a bell shape if there is no slip at the boundaries, i.e., a true Poiseuille flow. The present model of shear heating is more applicable in subduction channels and some extruding salt diapirs where the rheology is Newtonian viscous and pressure gradient drives extrusion.

Keywords Viscous dissipation · Newtonian fluid · Simple shear · Poiseuille flow

Introduction

Similar to ‘frictional heating’ in the brittle regime (Camacho et al. 2001; Ben-Zion and Sammis 2013), mechanical work that converts into heat during ductile shear is known

as ‘shear heating’, ‘viscous dissipation’, ‘viscous heating’, or ‘strain heating’ (Brun and Cobbold 1980; Nabelek and Liu 2004; Nabelek et al. 2010). Although deciphering shear heating from field-scale observations is not well established (Brun and Cobbold 1980; Vauchez et al. 2012), the heating could affect the thermal evolution of any nearby sedimentary basins. Such evolution paths are of practical interest, especially in the petroleum geosciences (Starin et al. 2000; Souche, internet reference).

Shear heating has been reported to attain significant magnitude when (1) the overthrust unit is thick (≥ 5 km; Brewer 1981); (2) the shear stress and the strain rate are high ($\sim 1,000$ MPa, 10^{-11} – 10^{-12} s $^{-1}$; Molnar and England 1990); (3) the slip/convergence rate is high (>1 cm year $^{-1}$; Graham and England 1976; Burg and Gerya 2005; more precisely ~ 4 cm year $^{-1}$; Nabelek and Liu 2004) as expected in subduction zones (review by Seyfert 1987); (4) deformation that takes place at a shallower depth (Hochstein and Regenauer 1998); (5) the shear zone material is ‘cold’ and rigid (Leloup et al. 1999); and (6) the sheared rock has a high viscosity and a high magnitudes of activation energy (Regenauer-Lieb and Yuen 2003). Shear heating may (Harris et al. 2000) or may not (Nabelek et al. 2010) be dependent on the distribution pattern of radioactive isotopes in the shear zones.

Shear zones can act as paths and source of melts by shear heating (Nabelek et al. 2010; review by Clark et al. 2011; but see Camacho et al. 2001 for counter arguments), which in collisional regimes is leucogranites (Nabelek and Liu 1999; Nabelek and Liu 2004; Nabelek et al. 2011). Had there been partial melting (‘thermal softening’: Brun and Cobbold 1980), further shear heating would have decreased, and the buoyant melt would have extruded leading to further heating. Subsequent melting could extrude the melt in a second pulse, and the cycle may

S. Mukherjee (✉)
Department of Earth Sciences, Indian Institute of Technology
Bombay, Powai, Mumbai 400 076, Maharashtra, India
e-mail: soumyajitm@gmail.com

K. F. Mulchrone
Department of Applied Mathematics, School of Mathematical
Sciences, University College, Cork, Ireland

continue (Nabelek et al. 2010; also see Fig. 1 of Hobbs et al. 2011). The heating could be tectonically noteworthy by reducing the viscosity thereby enhancing the ongoing deformation (Fleitout and Froidevaux 1980); triggering large-scale earthquakes and micro-scale grain growth (Regenauer-Lieb and Yuen 2003; Keleman and Hirth 2007); localizing strain (Vauchez et al. 2012; but see Montési 2013 for reverse arguments); syn-kinematic magmatism in the lithospheric mantle (Vauchez et al. 2012); accelerating the exhumation rate of rocks from the lower crust by producing $0.1\text{--}1 \mu \text{Wm}^{-2}$ of heat prior to orogenic melting (Burg and Gerya 2005; Johnson and Harley 2012); and switching the deformation pattern in orogens, from buckling to thrusting for example (Burg and Schmalholz 2008).

Several 2D and 3D thermo-mechanical models in the last few decades have come up to explain terrain tectonics (e.g., Burg and Schmalholz 2008), viz. the Barrovian- and the inverted metamorphism, and the dynamics of subduction zones (Burg and Gerya 2005; Camacho et al. 2001 and references therein). Analytical modeling of shear heating of non-Newtonian ductile shear zones, not specific to simple shear, led Fleitout and Froidevaux (1980) to conclude that the mid-portion of the shear zone develops the highest temperature, and thermal conduction widens the shear zone leading to a progressive drop in shear stress. While clay gouge developed, coeval to brittle shear may modulate viscous dissipation. The situation does not arise in ductile shear zones since no gouge develops in the latter case.

Thus, this brief review (plus that given in Vanderhaeghe 2012) reveals that no geoscientific study to date has focused on shear heating of ductile rocks of simple Newtonian rheology. Unlike the pseudotachylites that are possibly the products of shear heating for brittle fault zones (review by Blenkinsop

2000), the physical manifestation of such heating during ductile deformation on semi-solid rocks is not well understood. Also, shear heating as a function of slip rates at the boundaries, pressure gradient, dip of the shear zone, density and viscosity of the rock are not available. This work aims to use these parameters to deduce shear heating from Newtonian ductile simple shear zones. Simple shear has recently been discussed for the ductile- and brittle regimes (Mukherjee and Koyi 2009; Mukherjee 2010a, b; Mukherjee 2011a, b; Mukherjee 2012a; Koyi et al. 2013 etc.).

Mathematical model

Formulation

A parallel-sided and dipping shear zone with very long and rigid boundaries containing an incompressible Newtonian viscous fluid is considered. A pressure gradient acts along the shear zone and comprises a component due to gravity tending down-dip flow of the fluid. The extrusive pressure gradient could occur due to density differences between the material in the shear zone and the surrounding material. Here, it is assumed that the gradient due to extrusion is of greater magnitude than that due to gravity, and overall, the gradient drives the fluid up-dip along the zone. In the case of a shear zone inclined to the horizontal by θ (Mukherjee and Mulchrone 2012), the pressure gradient due to gravity is given by $\rho_c g \sin \theta$ where ρ_c is the density of the material in the shear zone, and the pressure gradient due to extrusion is $\rho_b g \sin \theta$ due to the surrounding material of density ρ_b and g is acceleration due to gravity. Hence, the overall pressure gradient is $(\rho_b - \rho_c)g \sin \theta$ so that when $\rho_b > \rho_c$ extrusion overcomes gravity. The boundaries of the shear zone are considered to undergo reverse-sense simple shear so that the hanging wall block moves up relative to the footwall block.

Derivation

From continuum mechanics (Lautrup 2011, p. 262), the governing equation is:

$$\mu \frac{d^2 U_x(y)}{dy^2} = \frac{dp}{dx} \quad (1)$$

where μ is the viscosity of the material inside the shear zone, $U_x(y)$ is the velocity in the x -direction which varies only with y , and $\frac{dp}{dx}$ is the pressure gradient along the channel. The pressure gradient is a constant as follows:

$$\frac{dp}{dx} = -G \quad (2)$$

where G encapsulates the gradient due to gravity and extrusion, i.e., for positive G motion takes place in the

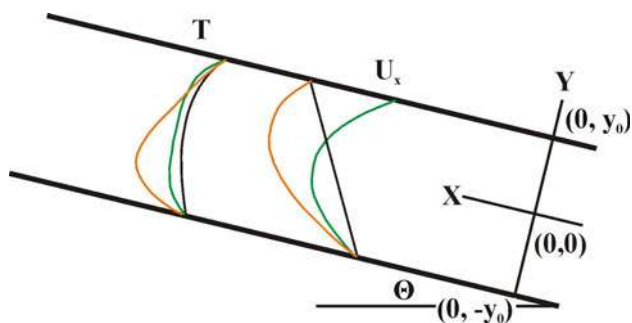


Fig. 1 A simple shear zone of Newtonian rheology and parallel boundaries that dip at an angle of θ . Shear velocity (U_x) is plotted along the X -axis across the shear zone (along the Y -direction). *Green profile* pressure gradient induced flow with stationary boundaries. *Black profile* boundaries slipping with a reverse shear sense under zero resultant pressure gradient. *Orange profile* boundaries slipping with a reverse sense and at the same time a resultant pressure gradient pushes the fluid up-dip. For these flow types, the temperature (T) profiles are shown in respective colors. See the main text for discussion

positive x -direction (see Fig. 1) so that extrusion overcomes gravity and vice versa for negative G . Taking $G = (\rho_b - \rho_c)g \sin \theta$ so that when $\rho_b > \rho_c$ then $G > 0$ and extrusion overcomes gravity.

The shear zone is of width $2y_0$ with the x -axis parallel to the shear zone boundary and placed equidistant from the boundaries. Solving Eq. 1 along with the boundary conditions that $U_x(y_0) = U_s$ and $U_x(-y_0) = 0$, the velocity profile is given by:

$$U_x(y) = \frac{G}{2\mu}(y_0^2 - y^2) + \frac{U_s}{2y_0}(y_0 + y) \tag{3}$$

(see the orange colored profile of U_x in Fig. 1). $U_s > 0$ results in a reverse shearing, whereas $U_s < 0$ results in normal shearing along the channel. If there is a need to model a shear zone where both boundaries are in motion (i.e., $U_x(y_0) = U_u$ and $U_x(-y_0) = U_l$), then one needs to consider $U_s = U_u - U_l$. Shear senses in these types of flow have been described in detail by Mukherjee (2012b, c).

The first component of the right hand side of Eq. 3 represents the motion due to Poiseuille flow and the second component represents motion due to Couette flow. Eq. 3 may be conveniently re-parameterized in terms of average velocities. The average velocity due to Poiseuille flow is:

$$V_p = \frac{1}{2y_0} \int_{-y_0}^{y_0} \frac{G}{2\mu}(y_0^2 - y^2) dy = \frac{Gy_0^2}{3\mu} \tag{4}$$

so that $G = \frac{3\mu V_p}{y_0^2}$, and the average velocity due to Couette flow is:

$$V_c = \frac{1}{2y_0} \int_{-y_0}^{y_0} \frac{U_s}{2y_0}(y_0 + y) dy = \frac{U_s}{2}$$

Hence, the velocity is as follows:

$$U_x(y) = \frac{3V_p}{2y_0^2}(y_0^2 - y^2) + \frac{V_c}{y_0}(y_0 + y) \tag{5}$$

The thermal effect of such a velocity profile is obtained from work rate associated with the velocity field (Mulchrone 2004; Turcotte and Schubert 2006; Lautrup 2011, p. 381) and is given by

$$\mu \left(\frac{dU_x}{dy} \right)^2 = \mu \left(\frac{V_c}{y_0} - \frac{3V_p y}{y_0^2} \right)^2 \tag{6}$$

Hence, the equation for temperature (T) in the steady state is:

$$k \frac{d^2 T}{dy^2} + \mu \left(\frac{V_c}{y_0} - \frac{3V_p y}{y_0^2} \right)^2 = 0 \tag{7}$$

subject to the boundary conditions $T(-y_0) = T_l$ and $T(y_0) = T_u$, which impose constant temperatures at the

lower and upper boundaries, respectively. k is the coefficient of thermal conductivity of the material inside the shear zone. Effectively, this means that heat is allowed to conduct in or out of the channel. The solution to Eq. 7 is:

$$T(y) = \left[\frac{1}{2} \left((T_u + T_l) + \frac{y}{y_0} (T_u - T_l) \right) + \frac{\mu V_c^2}{2k} \left(1 - \frac{y^2}{y_0^2} \right) + \frac{\mu V_c V_p y}{k y_0} \left(\frac{y^2}{y_0^2} - 1 \right) + \frac{3\mu V_p^2}{4k} \left(1 - \frac{y^4}{y_0^4} \right) \right] \tag{8}$$

The first term represents the steady-state temperature solution in the absence of viscous heating and demonstrates a linear variation in temperature from T_l to T_u from the lower to upper boundaries. The second term is the contribution due to Couette flow and the fourth term is due to Poiseuille flow. The third term is present only when both shearing and channel flow persists (see Mukherjee 2005 for the global debate on channel flow). Temperature profiles due to Couette or Poiseuille flow alone are symmetric, whereas when both flow types interact, the profile becomes asymmetric (see Fig. 1). The last three terms of Eq. 8 give the temperature rise due to shear heating.

Interpretation

Equation 8 reveals that shear heating depends on the following parameters: thermal conductivity (k), density (ρ_c) and viscosity (μ) of the rock material inside the shear zone, slip rate of the boundaries, position (y) inside the shear zone, and dip (θ) and thickness ($2y_0$) of the shear zone. The temperature distribution within the shear zone follows an asymmetric quartic curve when both Poiseuille and Couette flow occur inside the shear zone ($U_s = U_u - U_l$ indicates absolute movement direction similar to Goncharov et al. 2007) (see orange curve for temperature in Fig. 1). Whereas the velocity profile in this case has its vertex located within the upper portion of the shear zone, the maximum of the temperature profile lies within the bottom portion (compare orange curves of U_x and T in Fig. 1). This is to be expected since the maximum of the velocity profile represents the point of minimum shear strain. Away from the velocity maximum shear strain increases. The temperature profile is independent of duration of shearing since no time parameter occurs in Eq. 8; however, this is because the derivation inherently assumes that the temperature has reached the steady state. Further, shear heating is inversely proportional to the thermal conductivity for any orientation of the shear zone. The faster the average velocities (V_c and V_p in Eq. 8) in the shear zone, the more vigorous is the shear heating, proportional in general to the square of the velocity. This is consistent with Burg and Gerya's (2005) conclusion that a higher slip/convergence rate between

plates produces higher temperatures. On the other hand, shear heating is directly proportional to viscosity of the fluid. There is a nonlinear relationship between the dip (θ) of the shear zone and shear heating as evidenced from the relationship between V_p and θ ($(\rho_b - \rho_c)g \sin \theta = G = \frac{3\mu V_p}{y_0^2}$). These relations hold true for any location of the vertex and the pivot of the velocity profile (see Fig. 2a, b of Mukherjee 2012b for their locations).

The flow component due to a pressure gradient, i.e., Poiseuille flow vanishes when either (1) the gravity and the extrusive contributions to the pressure gradient counterbalance within the inclined shear zone (i.e., $\rho_b - \rho_c = 0$, equal densities) or (2) the shear zone is horizontal thus no pressure gradient exists (i.e., $\sin \theta = 0$). In these cases, $V_p = 0$ and the last two terms in Eq. 8 disappear. The temperature distribution inside the shear zone becomes symmetric and parabolic in this case with the maximum at the center of the shear zone. In other words, the central portion of the shear zone undergoes maximum heating (black profile of T in Fig. 1).

For a purely Poiseuille flow, i.e., when there is no relative motion of the shear zone boundaries ($V_c = 0$), and only a pressure gradient drives the fluid, $(\rho_b - \rho_c)g \sin \theta \neq 0$, the temperature distribution follows a symmetric quartic curve. There must exist a broad zone of elevated shear-related temperatures in the central zone. Near the boundaries, temperature drops abruptly and is zero at the boundaries (the green profile of T in Fig. 1).

Discussion and conclusions

Understanding viscous dissipation is of importance in deformation and extrusion mechanisms, orogeny, basin evolution and in the petroleum geosciences. For an inclined simple shear zone with Newtonian rheology where an updip density-driven pressure gradient overpowers the downdip gravity gradient along the shear zone, shear heating is a function of thermal conductivity, slip rate, position of measurement inside the zone, density and viscosity of the shear zone material, and dip and thickness of the shear zone. This model has the advantage over previous models of being able to take account of the extrusive pressure gradient that exists in many collisional orogens such as the Himalaya (Yin 2006) and the Grenville province (Rivers 2009). In general, the temperature due to shear heating peaks inside the shear zone and falls to zero at its boundaries. Shear heating intensifies when the total slip rate increases. A parabolic temperature profile is produced when there is no resultant pressure gradient. Shear heat is proportional to the square of the slip rate of the boundaries in that case. A flow driven solely by pressure gradient without slip along the boundaries leads to a broad zone of

uniform high temperature inside the shear zone. For an inclined shear zone with a reverse sense of movement and an upward resultant pressure gradient, the top portion of the zone attains maximum velocity, but the bottom portion a maximum temperature.

A number of thermo-mechanical models for orogenic shear zones (Kellett et al. 2010) take care of geothermal gradient, radioactive heat, thermal expansion coefficients, power law behavior, density changes due to mineral phase transition, extrusion augmented by focused erosion, vertical variation of viscosity, correlation between the width of the shear zone and depth, etc. (partially reviewed in Mukherjee 2012d). However, this work follows Mukherjee (2012b, c, d) and uses what are considered the minimum basic parameters (also see Mukherjee 2007; Mukherjee and Koyi 2010a, b; Mukherjee et al. 2012; Mukherjee 2013a). Besides, gravitational spreading of the extruded mass, kinematic dilatancy, strain partitioning, and temporal changes in mechanical behavior of rocks were also ignored. Equation 8 can also describe temperature profiles when (1) there is a normal sense of ductile shear and/or the resultant pressure gradient drives the fluid downdip and (2) the shear zone is horizontal.

Ductile shear zones at depth are dominated by simple shear (Vauchez et al. 2012; Mukherjee 2013b). Therefore, investigation of viscous dissipation in simple shear is important. Shear zones in some cases, e.g., subduction channels (Gerya and Stöckhert 2006; Mukherjee and Mulchrone 2012), and extruding salt diapirs (Bruthans et al. 2006; Mukherjee et al. 2010) behave as Newtonian viscous fluids. In those cases, the presented model is most applicable. However, many natural shear zones consist of a significant pure shear component (e.g., sub-simple shear zones/general shear zones) (review by Xypolias 2010). The present shear heat model cannot be applied directly to these cases. A more general shear heating model is required to decipher the relative role of simple shear in the case of general shear. Can shear heating explain abnormal geothermal gradients observed in some shear zones (such as Montomoli et al. 2013)?

Acknowledgments SM was supported by the Department of Science and Technology (New Delhi), Grant Number: IR/S4/ESF-16/2009(G). Discussions with Djordje Grujic (Dalhousie University) were very fruitful. Chief Editorial handling: Christian Dullo. Managing Editorial works: his wife Monika Dullo. Paris Xypolias (University of Patras) is thanked for providing a positive review. Chris Talbot (retired from Uppsala University) helped improve the English as an informal reviewer in an earlier version.

References

- Ben-Zion Y, Sammis CG (2013) Shear heating during distributed fracturing and pulverization of rocks. *Geol* 41:139–142
- Blenkinsop TG (2000) Deformation microstructures and mechanisms in minerals and rocks. Springer, Berlin

- Brewer J (1981) Thermal effects of thrust faulting. *Earth Planet Sci Lett* 56:233–244
- Brun JP, Cobbold PR (1980) Strain heating and thermal softening in continental shear zones: a review. *J Struct Geol* 2:149–158
- Bruthans J, Fillipi M, Geršl M et al (2006) Holocene marine terraces on two salt diapirs in the Persian Gulf, Iran: age, depositional history and uplift rates. *J Quat Sci* 21:843–57
- Burg J-P, Gerya T (2005) The role of viscous heating in Barrovian metamorphism of collisional orogens: thermomechanical models and application to the Lepontine Dome in the Central Alps. *J Metamorph Geol* 23:75–95
- Burg J-P, Schmalholz SM (2008) Viscous heating allows thrusting to overcome crustal-scale buckling: Numerical investigation with application to the Himalayan syntaxes. *Earth Planet Sci Lett* 274:189–203
- Camacho A, McDougall I, Armstrong R et al (2001) Evidence of shear heating, Musgrave Block, central Australia. *J Struct Geol* 23:1007–1013
- Clark C, Fitzsimons ICW, Healy D et al (2011) How Does the Continental Crust Gets Really Hot?. *Elements* 7:235–240
- Fleitout L, Froidevaux C (1980) Thermal and mechanical evolution of shear zones. *J Struct Geol* 2:159–164
- Gerya T, Stöckhert B (2006) Two-dimensional numerical modeling of tectonic and metamorphic histories at active continental margins. *Int J Earth Sci* 95:250–274
- Graham CM, England PC (1976) Thermal regimes and regional metamorphism in the vicinity of overthrust faults: an example of shear heating and inverted metamorphic zonation from southern California. *Earth Planet Sci Lett* 31:142–152
- Harris N, Vance D, Ayres M (2000) From sediment to granite: timescales of anatexis in the upper crust. *Chem Geol* 162:155–167
- Hobbs BE, Ord A, Regenauer-Lieb K (2011) The thermodynamics of deformed metamorphic rocks: a review. *J Struct Geol* 33:758–818
- Hochstein MP, Regenauer-Lieb K (1998) Heat generation associated with collision of two plates: the Himalayan geothermal belt. *J Volcanol Geotherm Res* 83:75–92
- Johnson MRW, Harley SL (2012) Orogenesis: the making of mountains. Cambridge University Press, Cambridge, pp 1–388
- Keleman PB, Hirth G (2007) A periodic shear-heating mechanism for intermediate-depth earthquakes in the mantle. *Nature* 446:787–790
- Kellett DA, Grujic D, Warren C et al (2010) Metamorphic history 490 of a syn-convergent orogen parallel detachment: the South Tibetan detachment system, Bhutan Himalaya. *J Metamorph Geol* 28:785–808
- Koyi H, Schmeling H, Burchardt S et al (2013) Shear zones between rock units with no relative movement. *J Struct Geol* (in press)
- Lautrup B (2011) Physics of continuous matter, 2nd edn. Taylor & Francis, UK, p 262
- Leloup PH, Ricard Y, Battaglia J et al (1999) Shear heating in continental strike-slip shear zones: model and field examples. *Geophys J Int* 136:19–40
- Molnar P, England P (1990) Late Cenozoic Uplift of mountain ranges and global climate change: chicken or egg?. *Nature* 346:29–34
- Montési LGJ (2013) Fabric development as the key for forming ductile shear zones and enabling plate tectonics. *J Struct Geol* (in press)
- Montomoli C, Carosi R, Visonà D (2013) The south Tibetan detachment system: thermal and mechanical transition from deeper to upper structural levels. *Geophys Res Abstr* 15:EGU2013-6589 (European Geosciences Union General Assembly)
- Mukherjee S (2005) Channel flow, ductile extrusion and exhumation of lower-middle crust in continental collision zones. *Curr Sci* 89:435–436
- Mukherjee S (2007) Geodynamics, deformation and mathematical analysis of metamorphic belts of the NW Himalaya. Unpublished Ph.D. thesis. Indian Institute of Technology Roorkee, India, p 1-267
- Mukherjee S (2010a) Structures at Meso- and Micro-scales in the Sutlej section of the Higher Himalayan Shear Zone in Himalaya. *e-Terra* 7:1-27
- Mukherjee S (2010b) Microstructures of the Zaskar Shear Zone. *Earth Sci India* 3:9-27
- Mukherjee S (2011a) Mineral fish: their morphological classification, usefulness and shear sense indicators and genesis. *Int J Earth Sci* 100:1303–1314
- Mukherjee S (2011b) Flanking microstructures of the Zaskar Shear Zone, western Indian Himalaya. *YES Bull* 1:21-29
- Mukherjee S (2012a) Tectonic Implications and Morphology of Trapezoidal Mica Grains from the Sutlej section of the Higher Himalayan Shear Zone, Indian Himalaya. *J Geol* 120:575-590
- Mukherjee S (2012b) Simple shear is not so simple! Kinematics and shear senses in Newtonian viscous simple shear zones. *Geol Mag* 149:819–826
- Mukherjee S (2012c) Kinematics of “top-to-down” simple shear model in a Newtonian viscous rheology. *J Indian Geophys Union* (in press)
- Mukherjee S (2012d) Channel flow extrusion model to constrain dynamic viscosity and Prandtl number of the Higher Himalayan Shear Zone. *Int J Earth Sci* (in press)
- Mukherjee S (2013a) Higher Himalaya in the Bhagirathi section (NW Himalaya, India): its structures, backthrusts and extrusion mechanism by both channel flow and critical taper mechanisms. *Int J Earth Sci* (in press)
- Mukherjee S (2013b) Deformation Microstructures in Rocks. Springer, New York (in press)
- Mukherjee S, Koyi HA (2009) Flanking microstructures. *Geol Mag* 146:517-526
- Mukherjee S, Koyi HA (2010a) Higher Himalayan Shear Zone, Sutlej section: structural geology and extrusion mechanism by various combinations of simple shear, pure shear and channel flow in shifting modes. *Int J Earth Sci* 99:1267-1303
- Mukherjee S, Koyi HA (2010b) Higher Himalayan Shear Zone, Zaskar Indian Himalaya- microstructural studies & extrusion mechanism by a combination of simple shear and channel flow. *Int J Earth Sci* 99:1083–1110
- Mukherjee S, Mulchrone KF (2012) Estimating the Viscosity of the Tso Moriri Gneiss Dome, western Indian Himalaya. *Int J Earth Sci* 101:1929–1947
- Mukherjee S, Koyi HA, Talbot CJ (2012) Implications of channel flow analogue models for extrusion of the Higher Himalayan Shear Zone with special reference to the out-of-sequence thrusting. *Int J Earth Sci* 101:253-272
- Mukherjee S, Talbot CJ, Koyi HA (2010) Viscosity estimates of salt in the Hormuz and Namakdan salt diapirs, Persian Gulf. *Geol Mag* 147:497–507
- Mulchrone KF (2004) Discussion on “Flattening in shear zones under constant volume: a theoretical evaluation” by N. Mandal, C. Chakraborty and S. Samanta. [*J Struct Geol* 23: 1771–1780]. *J Struct Geol* 26:197–200.
- Nabelek PI, Hofmeister AM, Whittington AG (2011) The influence of temperature-dependent thermal diffusivity on the conductive cooling rates of plutons and temperature-time paths in contact aureoles. *Earth Planet Sci Lett* 317(318):157–164
- Nabelek PI, Liu M (1999) Leucogranites in the Black Hills of South Dakota: the consequence of shear heating during continental collision. *Geology* 27:523–526
- Nabelek PI, Liu M (2004) Petrologic and thermal constraints on the origin of leucogranites in collisional orogens. *Tran R Soc Edinb Earth Sci* 95:73–85

- Nabelek PI, Whittington AG, Hofmeister AM (2010) Strain heating as a mechanism for partial melting and ultrahigh temperature metamorphism in convergent orogens: Implications of temperature dependent thermal diffusivity and rheology. *J Geophys Res* 115:B12417
- Rivers T (2009) The Grenville province as a large hot long-duration collisional orogen—insights from the spatial and thermal evolution of its orogenic fronts. In: Murphy JB, Keppie JD, Hynes AJ (eds.) *Ancient orogens and modern analogues*. *Geol Soc Lond Spec Publ* 327:405–444
- Souche A (Internet reference) The thermal evolution in sedimentary basins above large shear zones and detachments—Biannual report VISTA 2011. <http://www.vista.no/binfil/download.php?tid=49993> (Accessed on 03 Jan 2012)
- Regenauer-lieb K, Yuen DA (2003) Modeling shear zones in geological and planetary sciences: solid- and fluid-thermal-mechanical approaches. *Earth Sci Rev* 63:295–349
- Seyfert CK (1987) Plate Tectonics, Mantle Plumes, and the Generation of Magmas. In: Seyfert CK (Ed.) *Encyclopedia of structural geology and tectonics*. Von Nostrand Reinhold Company, New York, pp 560–634 (*Encyclopedia of Earth Sciences* 10)
- Starin L, Yuen DA, Bergeron SY (2000) Thermal evolution of sedimentary basin formation with variable thermal conductivity. *Geophys Res Lett* 27:265–268
- Turcotte DL, Schubert G (2006) *Geodynamics*, 2nd ed. Cambridge University Press, Cambridge, pp 283–285
- Vauchez A, Tommasi A, Mainprice D (2012) Faults (shear zones) in the Earth's mantle. *Tectonophysics* 558(559):1–27
- Xypolias P (2010) Vorticity analysis in shear zones: a review of methods and applications. *J Struct Geol* 32:2072–2092
- Yin A (2006) Cenozoic tectonic evolution of the Himalayan orogen as constrained by along-strike variation of structural geometry, exhumation history, and foreland sedimentation. *Earth Sci Rev* 76:1–131